Received: 23 June 2020 | Revised: 9 September 2020 | Accepted: 28 September 2020

DOI: 10.1002/er.6094

RESEARCH ARTICLE

INTERNATIONAL JOURNAL OF ENERGY RESEARCH WILEY

Dual-purpose thermal management of Li-ion cells using solid-state thermoelectric elements

Amirhossein Mostafavi | **Ankur Jain**

Mechanical and Aerospace Engineering Department, University of Texas at Arlington, Arlington, Texas

Correspondence
Ankur Jain, Mechanical and Aerospace Engineering Department, University of Texas at Arlington, 500 W First St, Rm 211, Arlington, Texas 76019.
Email: jaina@uta.edu

Summary

Li-ion cells are used for energy storage and conversion in multiple applications, including electric vehicles and renewable energy. Unfortunately, Li-ion cells are very temperature sensitive. A high-rate discharge may result in significant heat generation, which, if not properly managed, may lead to overheating and thermal runaway. On the other hand, operation in low temperature ambient results in significant performance degradation. Most thermal management approaches investigated in the past do not address both cooling and heating requirements for a Li-ion cell. This paper investigates dual-purpose thermal management of a Li-ion cell using solid-state thermoelectric elements. Experiments show that a thermoelectric element can effectively cool down a cell, resulting in negligible surface temperature rise up to 5C discharge rate. By simply reversing the polarity of thermoelectric current, the same thermoelectric element is shown to cause rapid heating of the cell in a low temperature ambient. Experiments show that in a 0°C ambient, the cell surface temperature rises to 20°C within 10 s with 1.5A thermoelectric current. Experimental data are shown to be in good agreement with a numerical simulation model. Even though high power consumption and cost may be important concerns, the seamless switching between heating and cooling functions makes thermoelectric elements an attractive option for thermal management of Li-ion cells in specific applications.

KEYWORDS

Li-ion cells, thermal management, thermal runaway, thermoelectric effect

1 | INTRODUCTION

The intermittent nature of renewable energy sources such as solar and wind power necessitates a robust mechanism for energy storage. A number of different energy storage technologies have been investigated in the past, including sensible and latent thermal energy storage,[1] thermochemical energy storage,[2] electrochemical energy storage,[3] etc. Among these, electrochemical energy storage in Li-ion based cells and battery packs offers several advantages, such as compact energy storage, high discharge rates, etc. As a result, Li-ion cells have been widely investigated for electrochemical energy storage, in addition to applications in consumer electronics, electric vehicles, and military applications.[4] Overheating of Li-ion cells during energy conversion and storage processes presents a key technological challenge that affects both performance and safety.[5,6] Heat generated in a Li-ion cell during charge or discharge leads to significant temperature rise due to its poor thermal conductivity.[7] If the temperature exceeds a certain threshold, a series of cascading exothermic decomposition reactions occur that result in

ever-increasing cell temperature, eventually leading to fire and explosion.[8] Manufacturers often specify a maximum permissible temperature in the range of 60-70°C to avoid thermal runaway.

On the other hand, low temperature operation of Li-ion cells is also undesirable, as it has been shown to reduce performance and lifetime.[9] A Li-ion cell at low temperature must be rapidly heated up to an optimum window of 15-35°C. This is a particularly important consideration for Li-ion cells in an electric vehicle that may be required to rapidly start and operate in cold climates.

As a result of these considerations, a robust, dual-purpose thermal management system is critically important for the performance and safety of Li-ion cells. The thermal management system must be able to limit cell temperature rise due to heat generation during charge/discharge. It must also be able to rapidly heat up the cell from a low temperature ambient. Ideally, the same thermal management technique must be able to address both heating and cooling requirements, with seamless switching between the two modes.

A number of different approaches have been demonstrated separately for cell cooling and heating. Cooling approaches include air and liquid cooling,[10] heat pipes,[11] phase change cooling,[12] and thermoelectric cooling.[13] Air cooling is typically easiest to implement, but may not be effective in aggressive conditions. Studies on air cooling systems have mainly focused on optimization of flow configuration and cell layout. Results of a parametric study on staggered battery pack identified top-located airflow inlet and outlet as the best cooling strategy.[14] A reciprocating air flow pattern including forward and backward cycles was proposed to optimize temperature distribution of a single pouch cell.[15] Compared to air cooling, liquid cooling systems remove more heat, but are more complicated and required greater power.[16] Experiments on thermal silica plates integrated with water tubes show significant increase in cooling capacity and reduction in maximum temperature of the battery module.[17] Many other papers have also reported on optimization of cold plates for water cooling battery thermal management systems.[16,18,19] Phase change and heat pipe-based thermal management systems offer the advantage of being passive in nature.[20] In order to heat up a cell in a cold climate, Joule heating in a metal foil inserted in the cell has been shown to result in rapid self-heating.[21] Self-heating using alternate current passed through the cell has also been proposed.[22] Most thermal management approaches investigated in the past, including the literature cited above, do not simultaneously address both cooling and heating requirements of a Li-ion cell.

Thermoelectric-based thermal management may be an attractive approach for Li-ion cells because of the dual ability to remove heat from and pump heat into the cell as needed. Thermoelectric modules are solid-state heat pumps that produce a directional heat flow in response to an applied potential difference based on Peltier effect.[23] A standard single stage thermoelectric module consists of N-type and P-type semiconductor junctions connected electrically in series and thermally in parallel.[24] A potential difference applied across the device results in the flow of heat from one face to the other. Reversing the polarity of the potential difference results in reversal of direction of heat flow, and therefore, heat can be either removed or pumped into the system of interest. Performance of a thermoelectric element is characterized by the figure of merit, which is governed by the Seebeck coefficient, electrical conductivity, and thermal conductivity of the thermoelectric element. Bismuth telluride (Bi_2Te_3) alloys are widely used bulk material in commercial thermoelectric elements.[25] Thermoelectric elements offer reliable and passive operation, with no moving parts, but often suffer from high power consumption due to low figure of merit.[26]

Despite the high power consumption, a thermoelectric element may be suitable for Li-ion cell thermal management for niche applications where cooling during charge/discharge and heating in a low temperature ambient are both critical needs. While thermoelectric elements have been used widely for heating and cooling, their application for thermal management of Li-ion cells is somewhat limited. Most available literature focuses on numerical simulations rather than experimental measurements. More importantly, the dual use of thermoelectric elements for cooling and heating of Li-ion cells has not been recognized and investigated in the past. Numerical simulation of thermoelectric cooling has been compared to experimental data in the context of cooling of battery pack of an electrical vehicle.[27] In a related study, cooling of Lithium iron phosphate cells with thermoelectric element was evaluated.[28] Numerical simulation of a battery pack cooled by thermoelectric elements was carried out.[29] Heat exchanger design optimization was performed with numerical simulation of a battery cell cooled by thermoelectric modules.[30] In another paper, thermoelectric elements were used to cool down the heat transfer fluid that, in turn, cools a cylindrical heater that mimics a Li-ion cell.[31] Given the theoretical possibility of obtaining both cooling and heating effects by reversing the polarity of the thermoelectric current, thermoelectric elements may offer an attractive approach for dual-purpose thermal management of a Li-ion cell.

This paper presents experimental and numerical analysis of dual-purpose thermal management of a Li-ion polymer cell using thermoelectric elements. Excellent cooling of the cell at aggressive discharge rates, as well as

rapid heating of the cell in a low temperature ambient, are demonstrated by simply reversing the polarity of thermoelectric current. Experimental data are found to be in very good agreement with numerical simulations. These results demonstrate the capability of thermoelectric elements to simultaneously address two critical thermal management challenges in Li-ion cells. Experiments and numerical simulations are described in Sections 2 and 3, respectively. Section 4 discusses key results, including experimental measurements, comparison with numerical simulations and prediction of core temperature of Li-ion cell.

2 | EXPERIMENTS

All experiments are carried out on a Li-ion polymer cell manufactured by Skyrich Battery Company. The cell has 4000 mAh nominal capacity and 3.2 V nominal voltage. Cell dimensions are 51 mm by 140 mm by 5 mm thick. The thermoelectric elements used in this work are manufactured by Hebei I.T. (Shanghai) Co. The rated maximum current and voltage of each thermoelectric element are 6.4 A and 16.4 V, respectively. Since each thermoelectric element covers an area of around 40 mm by 40 mm, the Li-ion cell is covered by three thermoelectric elements on each face for full coverage. All thermoelectric elements are connected in series to an Extech Instruments DC power supply (model number 382270).

Figure 1 shows a picture of the first set of experiments in which the cooling effect of thermoelectric elements during high-rate cell discharge is characterized. In these experiments, a 9-fin aluminum heat sink, and a brushless DC fan are mounted on the hot side of the thermoelectric elements for heat removal to ambient air. The fans are powered by a 12 V Keysight E3644A power supply. The Li-ion cell is charged/discharged in room temperature ambient by a Kikusui PFX2512 battery charge/discharge controller that controls an electronic load PLZ14W and a power supply unit PWR800L for desired charge/discharge cycling of the cell. BPChecker3000 software is used for programming the charge/discharge cycle and for acquiring cell voltage and current data. Cell surface temperature is measured at two points using K-type thermocouples from Omega. Thermocouples are connected to a National Instruments NI-9213 data acquisition system controlled by LabVIEW software for temperature data acquisition. Three different

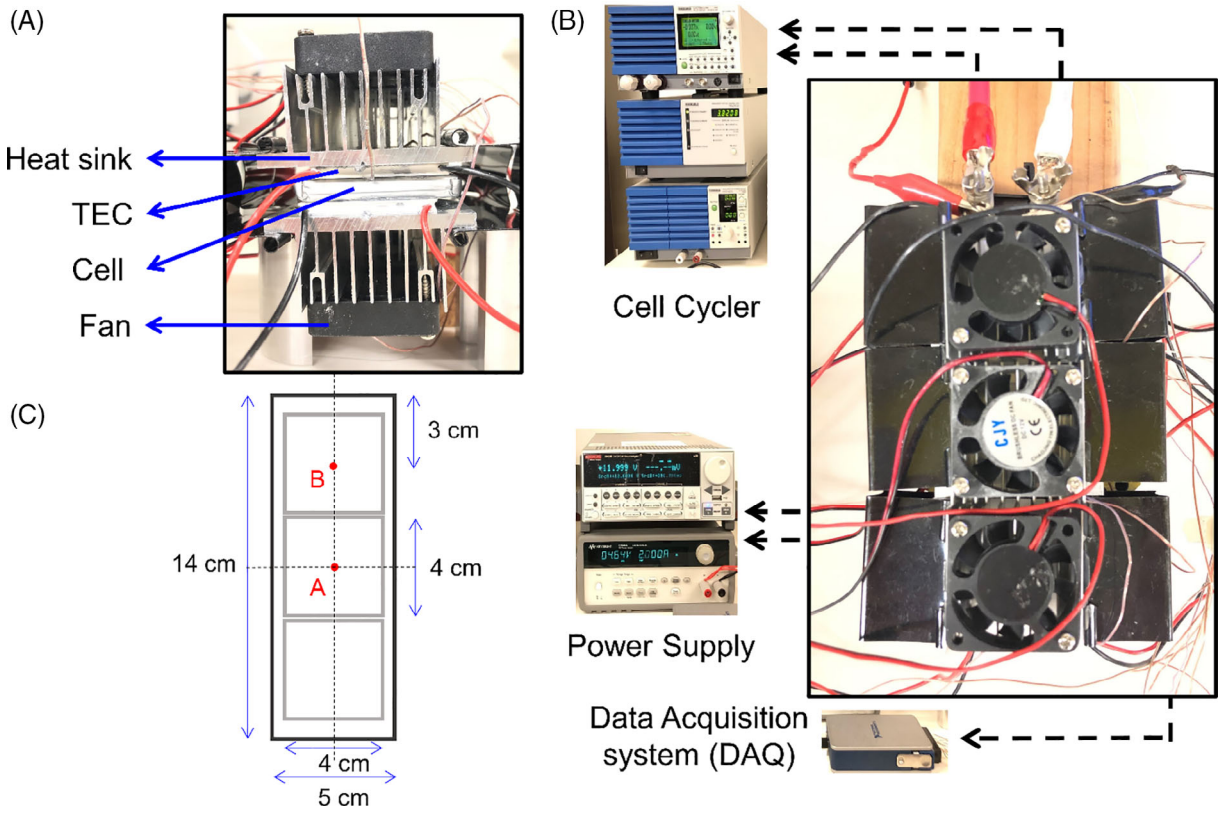

FIGURE 1 Pictures of the setup for thermoelectric-based cell cooling experiments: (A) and (B) show side-view and top-view pictures, respectively; (C) shows a schematic top view, including dimensions and thermocouple locations [Colour figure can be viewed at wileyonlinelibrary.com]

thermoelectric currents and two different discharge rates are investigated in these experiments.

In the second set of experiments, the heating up of the cell from a cold ambient by the thermoelectric elements is investigated. The cell is first kept inside a low temperature chamber long enough for thermal equilibration with the set temperature of the cold chamber, and then heated up by the thermoelectric elements. Current is passed through the thermoelectric elements with switched polarity, so that the side connected to the cell now serves as the hot side, and the thermoelectric elements effectively pump heat into the cell, as opposed to removing heat in the first set of experiments. Cell temperature data acquisition is carried out similar to the first set of experiments.

3 | SIMULATION MODELING

A finite-volume based heat transfer and fluid flow simulation is carried out in ANSYS Icepak software that numerically solves the equations governing thermal and fluid flow. These simulations serve to validate experimental measurements, as well as predict the core temperature of the cell, which is difficult to measure directly due to lack of access to the core of the cell. For these simulations, a model of the cell along with thermoelectric elements and heat sink, similar to the experimental setup shown in Figure 1A is placed inside a cabinet geometry. An opening with pressure outlet is modeled on the sides of the simulation domain. Continuity, momentum and energy equations govern incompressible flow and heat transfer in the simulation as follows:

$$\nabla.V = 0 \tag{1}$$

$$\rho\left(\frac{\partial V}{\partial t} + (V.\nabla)V\right) = -\nabla \mathrm{p} + \nabla.\tau + \rho \mathrm{g} \tag{2}$$

$$\rho c_p\left(\frac{\partial T}{\partial t} + (V.\nabla)T\right) = k\nabla^2 \mathrm{T} + \mathrm{Q} \tag{3}$$

where V, p, τ, and Q denote velocity vector, pressure, viscous stress tensor, and heat source term, respectively. ρ, c_p, k, and g are density, heat capacity, thermal conductivity, and acceleration due to gravity, respectively. Viscous dissipation is neglected in the energy equation. Associated boundary conditions include openings for inflow and outflow, while no-slip is defined at other boundaries.

The geometry of the cell, thermoelectric elements, heat sinks, and fans is modeled in order to closely match experimental conditions. The simulation domain is meshed with hex-dominant mesh elements. A total of 920 232 nodes are used. Further mesh refinement is found to result in negligible change in results. Values of thermal properties reported for a Li-ion polymer cell of the same chemistry and similar size as the present cell[32] are used in simulations. Thermal conductivity of the Li-ion cell is modeled to be anisotropic in nature, with values of 0.99 and 24.6 W m^{-1} K^{-1} in the through-plane (thickness) and in-plane directions, respectively. Specific heat capacity of the cell is taken to be 1050 J kg^{-1} K^{-1}, as reported by the same paper. Mass density of the cell is determined through measurements to be 2050 kg m^{-3}.

The value of heat generation rate as a function of C-rate has been reported in the past for a Li-ion polymer cell of the same chemistry and similar size as the cell in the present study.[32,33] These values of heat generation rate are used in simulations. Heat generation rate is expressed on a volumetric basis to account for the different capacities of the present cell and the one in the previous paper. Heat generation rate in the cell is assumed to remain constant during the discharge period.[34] The use of previously reported thermal parameters in these simulations is reasonable because the cell in the present has the same chemistry and similar size as the previously reported cell. Unfortunately, direct measurement of heat generation rate was not possible on the present cell.

Standard thermal properties of aluminum are used for the heat sink. Air speed from the fan is measured directly using an Extech 45118 anemometer and provided as a boundary condition for the simulations. Mixing length turbulent model is used for flow simulations, which is appropriate due to the fairly simple geometry and flow characteristics.[35] Radiative heat transfer is neglected due to the relatively small temperature rise. A fixed time step of 0.05 s is used throughout the computations, which are run for the entire charge/discharge duration. Residual convergence criterion is set to 10−5 for continuity and momentum equations, and 10−7 for energy equation. A library of different thermoelectric elements is available in the simulation tool. In each case, the values of thermoelectric element properties including Seebeck coefficient, electrical resistivity, and thermal conductivity are defined as third-order polynomial functions of absolute average temperatures between the cold and hot side. While such data for the specific thermoelectric elements used in present experiments are not directly available, values for a thermoelectric element from Laird Company, that has very close mechanical and thermal

properties compared to the present thermoelectric element, are used. Based on the expressions for temperature-dependent properties, the thermoelectric effect is simulated and combined with thermal and fluid flow calculations to predict temperatures of cold and hot sides of the thermoelectric element for a specified thermoelectric current. Considering the standard simplified energy equilibrium for a thermoelectric module, the cooling capacity Q_c can be described as

$$Q_c = \alpha I T_c - k(T_h - T_c) - 0.5RI^2 \quad (4)$$

where α, k, R, I, T_c, and T_h represent Seebeck coefficient, thermal conductance (W/K), resistance, current, cold side, and hot side temperatures of the TEC module, respectively. The input electrical power for the TEC module is given by

$$P_e = \alpha I(T_h - T_c) + RI^2 \quad (5)$$

which represents the sum of Joule heating and work done against the Seebeck effect.[24]

4 | RESULTS AND DISCUSSION

A number of experiments are carried out to characterize the cooling and heating aspects of thermoelectric-based thermal management. These experiments help understand the extent of cooling expected during high-rate discharge, as well as the capability of fast heating of a cell by operating the thermoelectric element in reverse polarity. Experimental data are compared with results from simulations described in Section 3.

4.1 | Cooling effect of thermoelectric elements

The Li-ion cell is discharged at 4C and 5C rates while being cooled by thermoelectric elements on both surfaces using the experimental methodology presented in Section 2. The cell surface temperature, measured at point A (see Figure 1C) is plotted as a function of depth of discharge (DOD) for 4C and 5C discharge rates in Figure 2A, B, respectively. During a discharge process, the value of DOD changes from 0.0 (fully charged) to 1.0 (fully discharged). In each case, three different thermoelectric cooling currents are used, and compared against the baseline case without thermoelectric cooling. Figure 2A shows that the cell surface temperature increases steadily during 4C discharge for the baseline line without thermoelectric cooling. In comparison, there is a significant reduction in temperature when the thermoelectric element is used. For each thermoelectric current, the cell surface temperature first reduces below ambient temperature and then slowly rises. Even at the end of the discharge process, the cell surface temperature is actually lower than the temperature at the start of the discharge process. Compared to the 20°C temperature rise in the baseline case, this is a very favorable thermal outcome.

The reason for the temperature dip in the initial period is that as the discharge process proceeds, the cell surface is first influenced by the cooling effect of the thermoelectric element, which begins as soon as thermoelectric current begins to flow. As expected, the extent of the initial temperature reduction is greater for higher thermoelectric currents. As time passes, diffusion of heat generated within the cell to the surface becomes more and more significant, causing an increase in temperature.

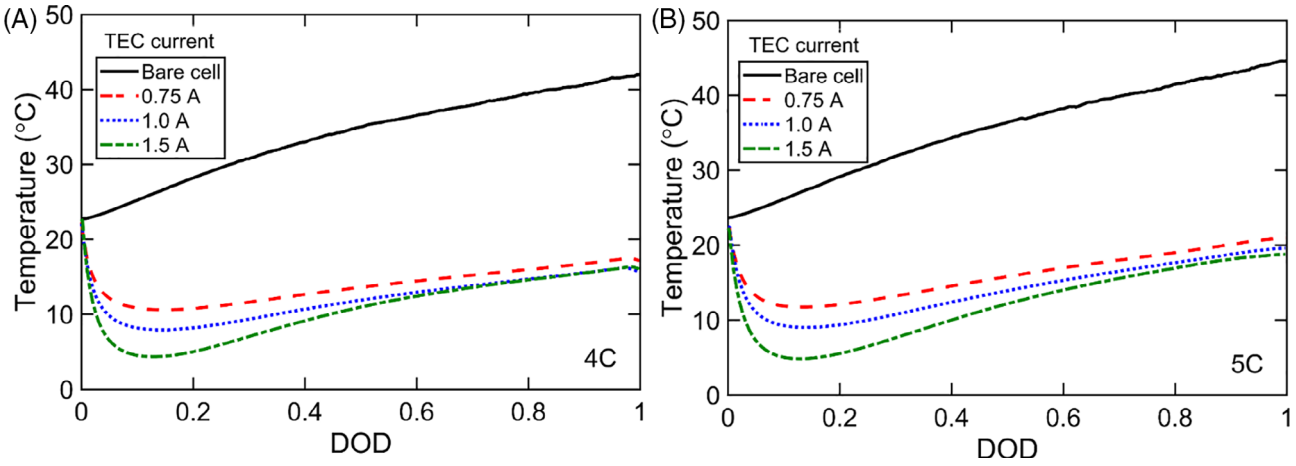

FIGURE 2 Cell surface temperature as a function of depth of discharge during thermoelectric-based cooling for (A) 4C and (B) 5C discharge rates. In each case, data are plotted for three different thermoelectric currents and the baseline case with no thermoelectric cooling [Colour figure can be viewed at wileyonlinelibrary.com]

While the thermoelectric cooling effect is near-instantaneous, in contrast, the heating effect of heat generation within the cell takes longer to reach the cell surface due to the finite diffusion timescale. This explains why the cell surface temperature first drops and then steadily rises with time. Cell surface temperature at the end of the process is largely invariant of the thermoelectric current.

The nature of measurements at 5C discharge rate shown in Figure 2B is consistent with the 4C data—cell surface temperature reduces first and then rises steadily. By comparing measurements with the baseline case, there is somewhat greater benefit of thermoelectric cooling (compared to the baseline) in the 5C case than in the 4C case.

These data show that thermoelectric cooling is very effective for thermal management during high rate discharge—there is nearly zero temperature rise at the surface compared to a temperature rise of 20-25°C for the baseline case without thermoelectric cooling. Note that the high power consumption of the thermoelectric elements may be a concern. The thermoelectric element is estimated to consume around 2.6 W power at 0.75 A current. Some strategies to minimize this power consumption may be possible. For example, experiments described here resulted in nearly zero temperature rise at 0.75A thermoelectric current. Depending on the application, it may be possible to tolerate a small temperature rise with the benefit of a lower thermoelectric current. Pulsed operation of thermoelectric elements may be another option for reducing power consumption.

4.2 | Heating effect in cold ambient

Fast heating of a Li-ion cell in a cold ambient is also an important thermal management need for practical applications. For example, in a cold environment, it is important to rapidly heat up the cells in an automotive battery pack to the optimal operating temperature range. This may be relevant, for example, when an electric car has been parked outside overnight in a very cold climate and the battery pack now needs to be rapidly heated up for optimal performance. By reversing the polarity of the thermoelectric element, it is possible to pump heat into the Li-ion cell instead of removing heat, and thereby help address this important thermal management requirement.

A number of experiments are carried out in order to characterize the thermoelectric heating effect on the Li-ion cell. In each case, the Li-ion cell, with thermoelectric elements attached on both faces is placed in a cold ambient for a long time. Once the cell has reached thermal equilibrium with its ambient, electric current is passed through the thermoelectric element with reversed polarity compared to experiments in Section 4.1, with the goal of providing heating to the cell, so that the optimal operating temperature can be reached as soon as possible. Three different thermoelectric currents are investigated at two different values of the cold ambient temperature. There is no charge/discharge of the cell during these experiments, since the goal is simply to characterize the impact of the thermoelectric element on heating up of the cell.

Figure 3A plots cell surface temperature at point A as a function of time for three different thermoelectric currents for a 0°C ambient. In each case, the cell temperature rises with time, with a greater rate of increase for larger thermoelectric currents. Taking 20°C as the target cell temperature, it is seen that it takes around 75 s for the cell to heat up when the thermoelectric current is somewhat low, at 0.75 A. At greater thermoelectric

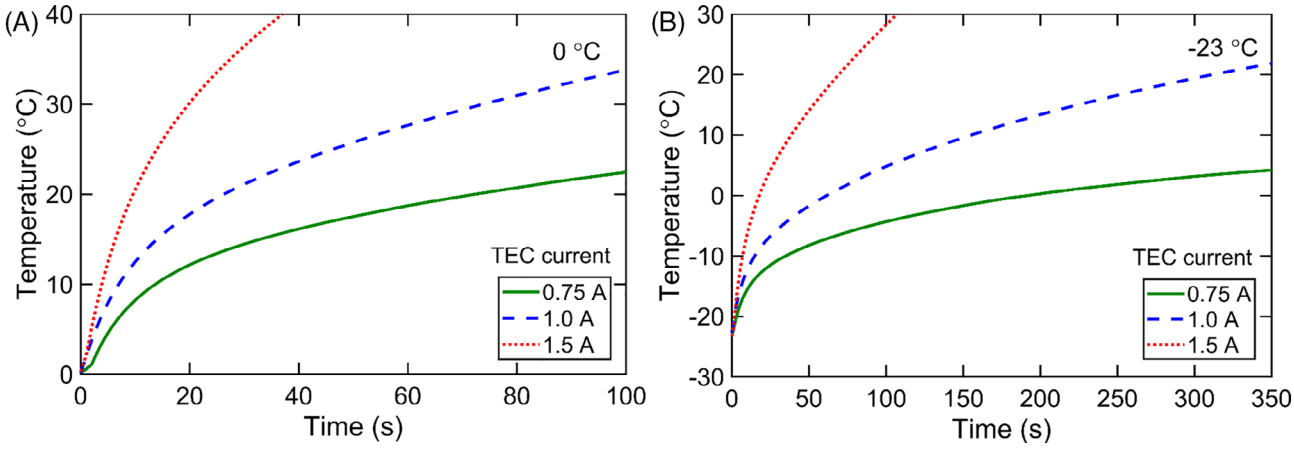

FIGURE 3 Cell surface temperature as a function of time during thermoelectric-based heating for (A) 0°C and (B) −23°C ambient temperature. In each case, data are plotted for three different thermoelectric currents, with polarity reversed compared to cooling experiments [Colour figure can be viewed at wileyonlinelibrary.com]

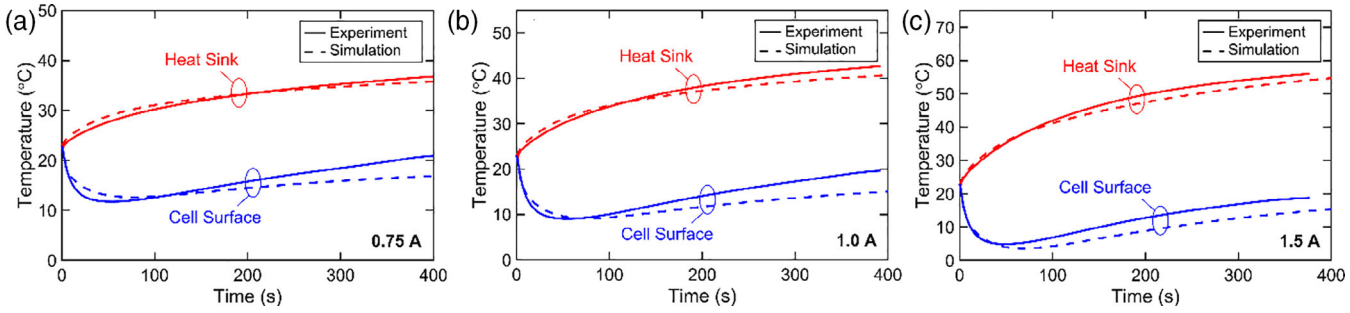

FIGURE 4 Comparison of experimental measurement and numerical simulation for cell surface and heat sink temperatures during 5C discharge for (A) 0.75A, (B) 1.0A, and (C) 1.5A thermoelectric current [Colour figure can be viewed at wileyonlinelibrary.com]

current, cell temperature rises much faster. For both 1.0 and 1.5 A cases, the cell reaches 20°C within 30 and 10 s, respectively, which is a relatively short duration.

In order to characterize the thermoelectric heating effect in even more stringent conditions, these experiments are repeated in a −23°C ambient. These results, plotted in Figure 3B show that with 1.5A thermoelectric current, optimal cell temperature is reached in about 70 s. As expected, at 1.0A thermoelectric current, the cell reaches 20°C after much longer, by around 310 s. With 0.75A thermoelectric current, the cell does not reach the optimal 20°C temperature at all, instead stabilizing at a lower temperature. These data are along expected lines, since a lower ambient temperature makes it more challenging to heat up the cell, and therefore, it takes longer time, and in some cases, the desired temperature is not reached at all.

It is quite significant that the desired temperature can be reached within 10 and 70 s for ambient temperatures of 0°C and −23°C, respectively with 1.5-A thermoelectric current. These data show that thermoelectric elements can help heat up a Li-ion cell into its optimal operating temperature range within a short time. Following initial warmup, the same thermoelectric element can be used for cooling the cell during charge/discharge by simply reversing the polarity of the thermoelectric current. This represents effective and seamless management of two key thermal challenges in a Li-ion cell.

Taken together, the data in Figures 2 and 3 demonstrate the dual benefit of thermoelectric elements. When the cell discharges at a high rate and therefore generates a lot of heat, thermoelectric elements may be an effective mechanism for thermal management, resulting in nearly zero temperature rise during discharge, while consuming relative low electrical energy. On the other hand, when the thermal requirement is to rapidly heat up the cell in a cold ambient, the same thermoelectric element, with reversed polarity can drive heat into the cell, thereby rapidly heating up the cell. Switching from one to the other merely requires changing the direction of the thermoelectric current. Even in fairly adverse ambient conditions, experiments demonstrate a relatively short time to heat up the cell with the thermoelectric element.

4.3 | Comparison of measurements with simulations

As discussed in Section 3, finite-volume simulations are carried out for comparison against experimental measurements.

Figure 4 compares temperature as a function of time obtained from experiments and simulations for a 5C discharge process at three different thermoelectric currents in the cooling mode. In each case, the cell surface temperature and heat sink temperature on the other face of the thermoelectric element are both plotted and compared. For each thermoelectric current, Figure 4 shows good agreement between experiments and simulations for both cell and heat sink temperatures. Simulations confirm the non-monotonic behavior of cell temperature over time due to the interplay between thermoelectric heat removal and diffusion of heat generated in the cell. As expected, temperature at the heat sink is greater than at the cell surface because in the cooling mode, the thermoelectric element pumps heat from the cell into the heat sink.

While Figure 4 plots the measured data at constant discharge rate for different thermoelectric currents, Figure 5 plots the measured data at constant thermoelectric current for different discharge rates. Cell surface and heat sink temperatures are plotted as functions of time for two different discharge rates in Figure 5A,B. In both cases, the current passing through the thermoelectric element is held constant at 1.0 A. Similar to Figure 4, there is good agreement between experimental measurements and finite-volume simulations. For both cell and heat sink temperatures, the nature of the experimentally measured curve is consistent with that predicted by simulations.

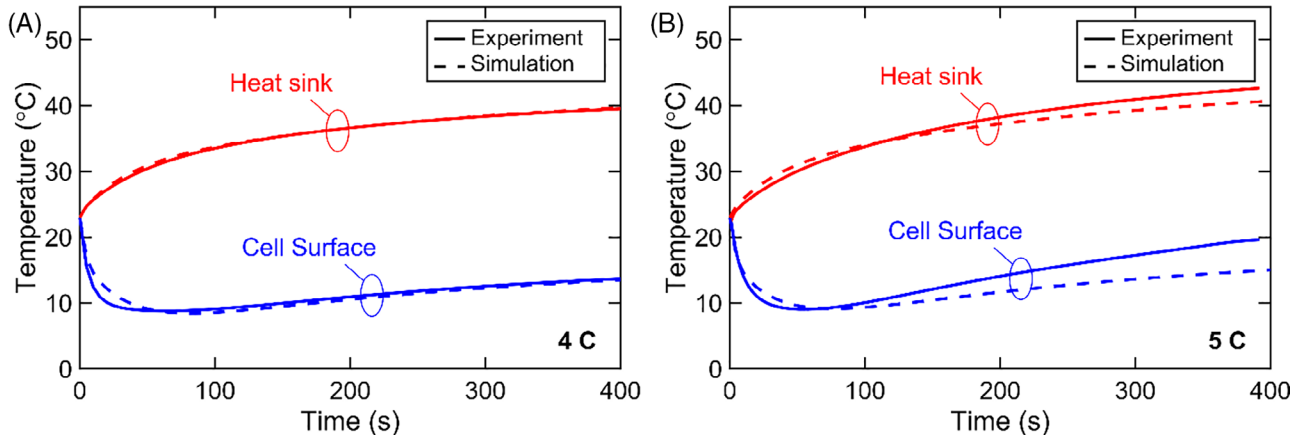

FIGURE 5 Comparison of experimental measurement and numerical simulation for cell surface and heat sink temperatures with 1.0A thermoelectric current for (A) 4C and (B) 5C discharge [Colour figure can be viewed at wileyonlinelibrary.com]

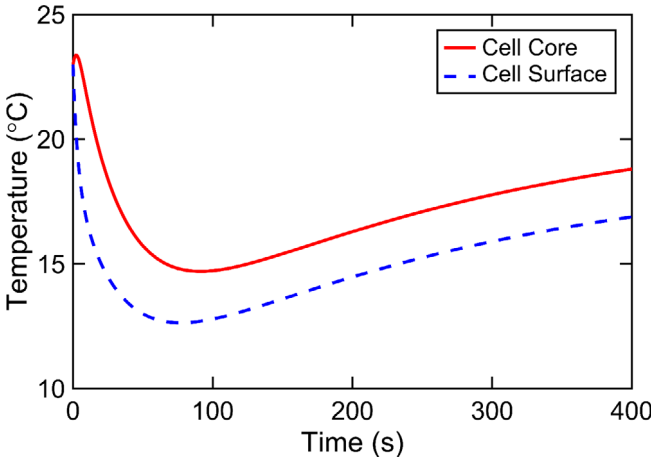

FIGURE 6 Core and surface cell temperatures predicted by numerical simulation for 5C discharge in the presence of cooling with 0.75A thermoelectric current [Colour figure can be viewed at wileyonlinelibrary.com]

There may be several reasons behind the relatively minor deviation between measurements and simulations in Figures 4 and 5. In addition to uncertainties in experimental measurement, the constant heat generation rate assumption during the discharge process may also be a source of error. Thermal contact resistance between components may play a small role, even though a thermal paste is used throughout to minimize thermal contact resistance.

4.4 | Core temperature estimation

Experimental data presented in Figure 2 show that the cell surface temperature may actually decrease during high rate discharge due to the cooling effect of the thermoelectric element. It is important to recognize that cooling impact of the thermoelectric element may be lesser at the core of the cell than at the cell surface, due to the large thermal resistance within the cell because of low thermal conductivity[7] and large interfacial thermal resistances within the cell.[36] In addition to the reported surface temperature measurements, it is important to quantify the impact of thermoelectric cooling on the core temperature of the cell.

Unfortunately, it is not possible to directly measure the core temperature of the cell since a temperature sensor may not be inserted into the hermetically sealed cell. While some methods for non-invasive core temperature estimation are available,[37] these methods may not be directly applicable here. In light of these difficulties, finite-volume simulations are carried out to predict the core temperature. There is high confidence in the simulation methodology due to good agreement with experimental measurements shown in Figures 4 and 5. Simulation results are presented in Figure 6 that plots predicted core and surface temperatures as functions of time for a 5C discharge process with 0.75A thermoelectric current. Figure 6 shows, as expected, that the cell core temperature is greater than the cell surface temperature. Figure 6 shows that while the cell surface temperature has a sharp drop followed by gradual rise, the core temperature increases for a very small time, followed by a reduction and finally, a gradual increase. This is explained on the basis of the balance between heat generation within the cell during discharge and heat removal by the thermoelectric element. There is a short period of temperature rise at the cell core due to heat generation being dominant until the cooling effect of the thermoelectric element diffuses from the cell surface to the cell core. This short period is consistent with the thermal penetration time calculated by thermal diffusion

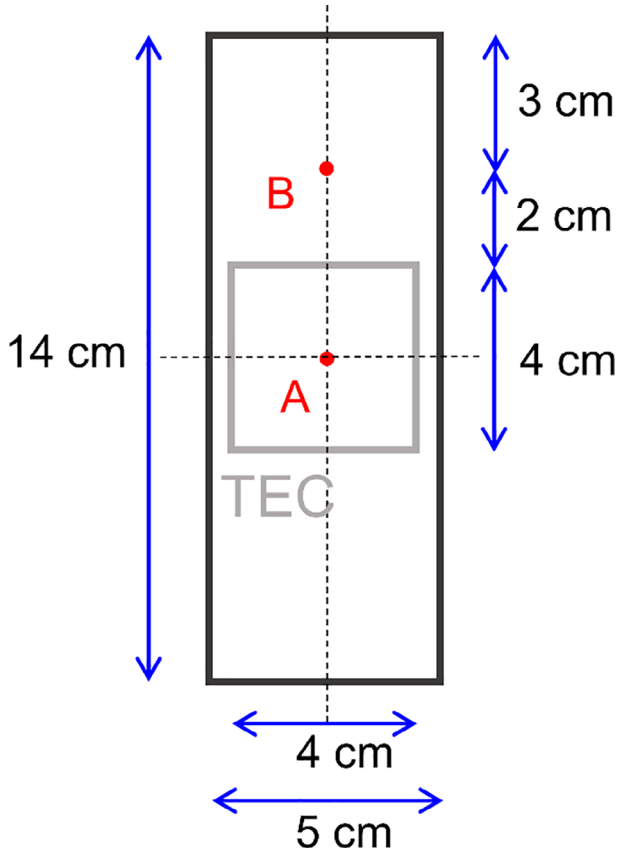

FIGURE 7 Schematic top view of thermoelectric cooling during partially disabled scenario. Only the middle thermoelectric element shown in this figure is active [Colour figure can be viewed at wileyonlinelibrary.com]

considerations. As the core begins to be influenced by the thermoelectric element, the core temperature begins to reduce. Eventually, heat generation and thermoelectric cooling balance each other out, and the core temperature rises again in a nearly linear fashion until the end of the discharge process. While Figure 6 shows greater temperature rise at the core compared to the surface, nevertheless, the net temperature rise during the entire process in the presence of thermoelectric cooling is negative even at the cell core.

4.5 | Effect of partial thermoelectric coverage

While experiments described above show effective thermal management of the Li-ion cell with thermoelectric elements, it is also important to understand the limits of thermoelectric cooling in practical scenarios. Specifically, the extent of cooling possible when the thermoelectric elements are operating partially must be studied. In order to do so, experiments are carried out where two of the three thermoelectric elements on each side of the Li-ion cell are considered to be inoperational by cutting off current supply. This mimics a practical scenario of partial failure of the thermoelectric-based thermal management system. The geometry for this case is shown in Figure 7, which indicates two locations A and B on the cell surface where temperature is measured. While point A is directly

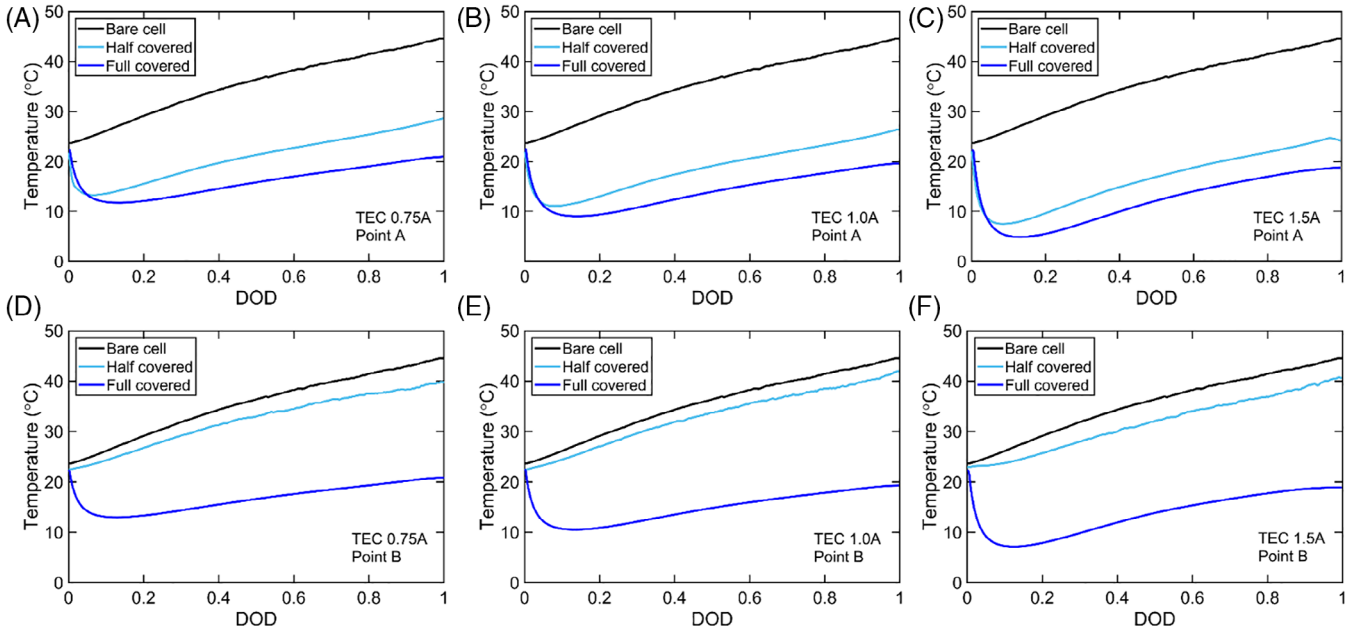

FIGURE 8 Comparison of cell surface temperatures at two different points for fully enabled and partially disabled scenarios for three different thermoelectric currents. (A)–(C) plot data for point A for 0.75, 1.0, and 1.5A thermoelectric currents. (D)–(F) present similar data for point B. In each case, the baseline temperature curve without thermoelectric cooling is also plotted for comparison [Colour figure can be viewed at wileyonlinelibrary.com]

under the single operational thermoelectric element, point B is under one of the failed thermoelectric elements.

Figure 8 summarizes temperature measurements at points A and B during discharge at 5C rate for fully covered and partially covered scenarios. Data are presented for three different thermoelectric currents. Figure 8A–C shows that thermal performance at point A in the partially covered case is nearly as good as the fully covered case. This is along expected lines, since point A lies directly underneath the single operating thermoelectric element, and therefore is not dramatically influenced by failure of the other thermoelectric elements. On the other hand, failure of two thermoelectric elements does have a more pronounced effect on temperature at point B, as shown in Figure 8D–F, even though temperature rise at point B is still lower than the baseline case. The behavior described above is consistent for all three thermoelectric currents investigated in these experiments. Figure 8 quantifies the effect of thermoelectric cooling in a scenario of partial operation.

5 | CONCLUSIONS

This paper shows that thermoelectric elements may offer an effective approach for simultaneously meeting the cooling and heating requirements for a Li-ion cell. Both cooling and heating of a Li-ion cell are demonstrated, with good agreement between experimental data and numerical simulation results. The seamless switching between cooling and heating modes by simply changing polarity of thermoelectric current makes this approach particularly attractive.

It is important to note that there may be significant energy consumption in the thermoelectric elements for thermal management of the Li-ion cell. At 0.75A thermoelectric current, the power consumption in the thermoelectric element is estimated to be 2.6 W. Even though the thermoelectric element is able to dissipate the energy it consumes to its hot side, and from there to the ambient by the heat sink and fan, nevertheless, the high power consumption of the thermoelectric element may be a concern for several applications. The trade-off between thermal management and power consumption is likely to be application-specific and needs to be carefully considered and optimized. Techniques for minimizing thermoelectric power consumption, such as those discussed briefly in Section 4.1, need to be investigated further. Despite the high power consumption and cost, thermoelectric elements may offer an attractive option for dual-purpose be suitable for thermal management of Li-ion cells in specific applications.

ACKNOWLEDGMENTS

This material is based upon work supported by CAREER Award No. CBET-1554183 from the National Science Foundation.

DATA AVAILABILITY STATEMENT

The data that support the findings of this study are available from the corresponding author upon reasonable request.

ORCID

Ankur Jain https://orcid.org/0000-0001-5573-0674

REFERENCES

1. Hasnain S. Review on sustainable thermal energy storage technologies. Part I: heat storage materials and techniques. *Energy Convers Manag*. 1998;39:1127-1138. https://doi.org/10.1016/s0196-8904(98)00025-9.
2. Cot-Gores J, Castell A, Cabeza LF. Thermochemical energy storage and conversion: A-state-of-the-art review of the experimental research under practical conditions. *Renew Sust Energ Rev*. 2012;16:5207-5224. https://doi.org/10.1016/j.rser.2012.04.007.
3. Shah K, Balsara N, Banerjee S, et al. State of the art and future research needs for multiscale analysis of Li-ion cells. *J Electrochem Energy Conv Storage*. 2017;14:1-17. https://doi.org/10.1115/1.4036456.
4. Scrosati B, Garche J. Lithium batteries: status, prospects and future. *J Power Sources*. 2010;195:2419-2430. https://doi.org/10.1016/j.jpowsour.2009.11.048.
5. Shah K, Vishwakarma V, Jain A. Measurement of multiscale thermal transport phenomena in Li-ion cells: a review. *J Electrochem Energy Conv Storage*. 2016;13:1-13. https://doi.org/10.1115/1.4034413.
6. Bandhauer TM, Garimella S, Fuller TF. A critical review of thermal issues in lithium-ion batteries. *J Electrochem Soc*. 2011;158:R1. https://doi.org/10.1149/1.3515880.
7. Drake S, Wetz D, Ostanek J, Miller S, Heinzel J, Jain A. Measurement of anisotropic thermophysical properties of cylindrical Li-ion cells. *J Power Sources*. 2014;252:298-304. https://doi.org/10.1016/j.jpowsour.2013.11.107.
8. Shah K, Jain A. Prediction of thermal runaway and thermal management requirements in cylindrical Li-ion cells in realistic scenarios. *Int J Energy Res*. 2019;43:1827-1838. https://doi.org/10.1002/er.4411.
9. Zhang S, Xu K, Jow T. The low temperature performance of Li-ion batteries. *J Power Sources*. 2003;115:137-140. https://doi.org/10.1016/s0378-7753(02)00618-3.
10. Chen D, Jiang J, Kim G-H, Yang C, Pesaran A. Comparison of different cooling methods for lithium ion battery cells. *Appl Therm Eng*. 2016;94:846-854. https://doi.org/10.1016/j.applthermaleng.2015.10.015.
11. Anthony D, Wong D, Wetz D, Jain A. Improved thermal performance of a Li-ion cell through heat pipe insertion. *J Electrochem Soc*. 2017;164:A961-A967. https://doi.org/10.1149/2.0191706jes.
12. Parhizi M, Jain A. Analytical modeling and optimization of phase change thermal management of a Li-ion battery pack. *Appl Therm Eng*. 2019;148:229-237. https://doi.org/10.1016/j.applthermaleng.2018.11.017.

13. Siddique ARM, Mahmud S, Heyst BV. A comprehensive review on a passive (phase change materials) and an active (thermoelectric cooler) battery thermal management system and their limitations. *J Power Sources*. 2018;401:224-237. https://doi.org/10.1016/j.jpowsour.2018.08.094.
14. Lu Z, Yu X, Wei L, et al. Parametric study of forced air cooling strategy for lithium-ion battery pack with staggered arrangement. *Appl Therm Eng*. 2018;136:28-40. https://doi.org/10.1016/j.applthermaleng.2018.02.080.
15. Wang S, Li K, Tian Y, Wang J, Wu Y, Ji S. Improved thermal performance of a large laminated lithium-ion power battery by reciprocating air flow. *Appl Therm Eng*. 2019;152:445-454. https://doi.org/10.1016/j.applthermaleng.2019.02.061.
16. Malik M, Dincer I, Rosen MA, Mathew M, Fowler M. Thermal and electrical performance evaluations of series connected Li-ion batteries in a pack with liquid cooling. *Appl Therm Eng*. 2018;129:472-481. https://doi.org/10.1016/j.applthermaleng.2017.10.029.
17. Wang C, Zhang G, Li X, et al. Experimental examination of large capacity $LiFePO_4$ battery pack at high temperature and rapid discharge using novel liquid cooling strategy. *Int J Energy Res*. 2017;42:1172-1182. https://doi.org/10.1002/er.3916.
18. Du X, Qian Z, Chen Z, Rao Z. Experimental investigation on mini-channel cooling-based thermal management for Li-ion battery module under different cooling schemes. *Int J Energy Res*. 2018;42:2781-2788. https://doi.org/10.1002/er.4067.
19. Li X, Zhou D, Zhang G, Wang C, Lin R, Zhong Z. Experimental investigation of the thermal performance of silicon cold plate for battery thermal management system. *Appl Therm Eng*. 2019;155:331-340. https://doi.org/10.1016/j.applthermaleng.2019.04.007.
20. Jaguemont J, Mierlo JV. A comprehensive review of future thermal management systems for battery-electrified vehicles. *J Energy Storage*. 2020;31:101551. https://doi.org/10.1016/j.est.2020.101551.
21. Yang X-G, Liu T, Wang C-Y. Innovative heating of large-size automotive Li-ion cells. *J Power Sources*. 2017;342:598-604. https://doi.org/10.1016/j.jpowsour.2016.12.102.
22. Zhang J, Ge H, Li Z, Ding Z. Internal heating of lithium-ion batteries using alternating current based on the heat generation model in frequency domain. *J Power Sources*. 2015;273:1030-1037. https://doi.org/10.1016/j.jpowsour.2014.09.181.
23. Huang B, Chin C, Duang C. A design method of thermoelectric cooler. *Int J Refrig*. 2000;23:208-218. https://doi.org/10.1016/s0140-7007(99)00046-8.
24. Enescu D, Virjoghe EO. A review on thermoelectric cooling parameters and performance. *Renew Sust Energ Rev*. 2014;38:903-916. https://doi.org/10.1016/j.rser.2014.07.045.
25. Champier D. Thermoelectric generators: a review of applications. *Energy Convers Manag*. 2017;140:167-181. https://doi.org/10.1016/j.enconman.2017.02.070.
26. Elsheikh MH, Shnawah DA, Sabri MFM, et al. A review on thermoelectric renewable energy: principle parameters that affect their performance. *Renew Sust Energ Rev*. 2014;30:337-355. https://doi.org/10.1016/j.rser.2013.10.027.
27. Alaoui C. Solid-state thermal management for lithium-ion EV batteries. *IEEE Trans Veh Technol*. 2013;62:98-107. https://doi.org/10.1109/tvt.2012.2214246.
28. Salameh Z, Alaoui C. Modeling and simulation of a thermal management system for electric vehicles. Paper presented at: 29th Annual Conference of the IEEE Industrial Electronics Society (IEEE Cat. No.03CH37468). (2003). doi:https://doi.org/10.1109/iecon.2003.1280100.
29. Liu Y, Yang S, Guo B, Deng C. Numerical analysis and design of thermal management system for lithium ion battery pack using thermoelectric coolers. *Adv Mech Eng*. 2014;6:852712. https://doi.org/10.1155/2014/852712.
30. Zhang C. Study on a battery thermal management system based on a thermoelectric effect. *Energies*. 2018;11:279. https://doi.org/10.3390/en11020279.
31. Lyu Y, Siddique A, Majid S, Biglarbegian M, Gadsden S, Mahmud S. Electric vehicle battery thermal management system with thermoelectric cooling. *Energy Rep*. 2019;5:822-827. https://doi.org/10.1016/j.egyr.2019.06.016.
32. Nieto N. A model-based design of a thermal management system for a high power Li-ion battery pack. (PhD dissertation). University of Navarra, San Sabastián; 2014.
33. Nieto N, Díaz L, Gastelurrutia J, et al. Thermal modeling of large format lithium-ion cells. *J Electrochem Soc*. 2013;160:A212-A217. https://doi.org/10.1149/2.042302jes.
34. Hallaj SA, Maleki H, Hong J, Selman J. Thermal modeling and design considerations of lithium-ion batteries. *J Power Sources*. 1999;83:1-8. https://doi.org/10.1016/s0378-7753(99)00178-0.
35. Dhinsa K, Bailey C, Pericleous K. Turbulence modelling for electronic cooling: a review. Paper presented at: 2005 International Symposium on Electronics Materials and Packaging; 2005. doi:https://doi.org/10.1109/emap.2005.1598275.
36. Vishwakarma V, Waghela C, Wei Z, et al. Heat transfer enhancement in a lithium-ion cell through improved material-level thermal transport. *J Power Sources*. 2015;300:123-131. https://doi.org/10.1016/j.jpowsour.2015.09.028.
37. Anthony D, Wong D, Wetz D, Jain A. Non-invasive measurement of internal temperature of a cylindrical Li-ion cell during high-rate discharge. *Int J Heat Mass Transf*. 2017;111:223-231. https://doi.org/10.1016/j.ijheatmasstransfer.2017.03.095.

How to cite this article: Mostafavi A, Jain A. Dual-purpose thermal management of Li-ion cells using solid-state thermoelectric elements. *Int J Energy Res*. 2021;45:4303–4313. https://doi.org/10.1002/er.6094